

Statistical visualisation of tidy and geospatial data in R via kernel smoothing methods in the `eks` package

Tarn Duong*

5 January 2023

Abstract

Kernel smoothers are essential tools for data analysis due to their ability to convey complex statistical information with concise graphical visualisations. Their inclusion in the base distribution and in the many user-contributed add-on packages of the R statistical analysis environment caters well to many practitioners. Though there remain some important gaps for specialised data types, most notably for tibbles (tidy data) within the tidyverse, and for simple features (geospatial data) within geospatial analysis. The proposed `eks` package fills in these gaps. In addition to kernel density estimation, which is the most widely implemented kernel smoother, this package also caters for more complex data analysis situations, such as density-based classification (supervised learning), mean shift clustering (unsupervised learning), density derivative estimation, density ridge estimation, and significance testing for density differences and for modal regions. We illustrate with experimental data how to obtain and to interpret the statistical graphical analyses for these kernel smoothing methods.

Keywords: classification, clustering, `ggplot2`, kernel density estimation, `sf`, simple features

1 Introduction

Kernel smoothers form an essential suite of statistical techniques for data analysis in the 21st century due to their ability to convey complex statistical information in a concise and intuitive visual format. This ability arises from their shared characteristic of transforming data samples into smoothed estimates. Kernel smoothers have provided insight in data analysis problems in many situations. A small recent selection of these includes: the identification of important biomedical functions, such as characterising different sub-cellular structures in single cells (Schauer et al., 2010) or characterising a single cell population in mixed cell samples (Chacón et al., 2011); the evaluation of predicted extreme temperatures to calibrate climate models (Béranger et al., 2019); the estimation of the home range of animal movements (Baíllo and Chacón, 2021); or the detection of traffic anomalies from traffic flows (Kalair and Connaughton, 2021). The most widely used kernel smoother is the kernel density estimate, which can be considered to be a smoothed version of the histogram. A major access point to kernel smoothers in the R statistical programming environment is the `ks` ('kernel smoothing') add-on package (Duong, 2007), which implements density estimation, classification (unsupervised learning), clustering (unsupervised learning), and inferential methods. This package utilises the base R graphics engine to generate its statistical graphics. Whilst it remains the most comprehensive graphics engine in

*Paris, France F-75000. Email: tarn.duong@gmail.com

R, the `ggplot2` graphics engine (Wickham, 2016) has gained popularity, as part of the ‘tidyverse’, especially with data analysis practitioners. Despite the dramatic rise in the number of analysis methods available in the tidyverse, nonetheless it comprises a limited range of natively implemented kernel smoothers. The first goal of the `eks` (‘extended kernel smoothing’) package (Duong, 2022) is to provide access to the comprehensive suite of kernel smoothers from the `ks` package in the tidyverse.

There is an analogous lack of kernel smoothers for geospatial data analysis. Existing R packages for geospatial analysis include `spatstat` (Baddeley and Turner, 2005) and `spatialEco` (Evans and Murphy, 2022). For these and similar packages, the underlying statistical framework are spatial point processes, rather than bivariate point clouds, as is for `eks`. This seemingly minor difference in the statistical framework has many consequences, since kernel-based data analyses, apart from kernel density estimates and intensity estimates, are rarely developed and implemented for spatial point processes. The geospatial functionality of the `eks` package is based on the the `sf` package (Pebesma, 2018), as it provides seamless geospatial functionality in R. Furthermore, the geospatial outputs in `eks` can be exported to external ‘Geographical Information Systems’ (GIS) software (such as ArcGIS and QGIS). This vastly expands the range of kernel smoothers available to geospatial analysts in a system which is familiar to them. The second goal of the `eks` package is to provide access to a comprehensive suite of kernel smoothers for geospatial analysis.

Thus a wide range of kernel smoothers is now available for tidy and geospatial data, and for `ggplot2` and base R graphical visualisations. The user is able to select and combine these components, with their differing strengths and applicabilities, in order to construct suitable data analysis workflows. To illustrate kernel smoothers for tidy and geospatial data, we employ the `grevilleasf` data set from the `eks` package, as shown in Figure 1. The full data set of 22203 plants from 238 different *Grevillea* species were collected in Western Australia. The south-west corner of Western Australia is one of the 25 ‘biodiversity hotspots’ which are ‘areas featuring exceptional concentrations of endemic species and experiencing exceptional loss of habitat’ identified in Myers et al. (2000) to assist in formulating priorities in biodiversity conservation policies.

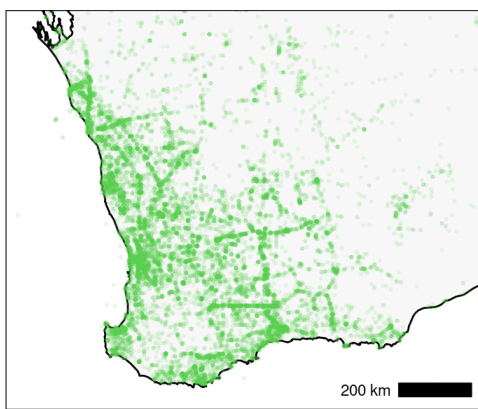


Figure 1: Scatter plot of the `grevilleasf` ($n = 22203$) data set, in the biodiversity hotspot of south-western Western Australia.

For brevity, we focus on this single data set as an example of both tidy and geospatial data. A tidy data set is a data matrix where (i) each variable forms a column and (ii) each observation

forms a row, and it is also known as a ‘long’ data set (Wickham, 2014). For our purposes in this paper, we refer to `grevilleasf_coord` solely as a tidy data set, and omit any mention of its geospatial characteristics, despite that its columns consist of 2-dimensional geographical coordinates. Similarly we refer to `grevilleasf` solely as a geospatial data set, and omit any mention of its tidy status, to emphasise its distinct geospatial characteristics.

```
R> grevilleasf_coord
  species      lon      lat
1  robusta 390106.5 6462671
2  speciosa 382689.2 6457387
3  robusta 390089.8 6462603
...
R> grevilleasf
Simple feature collection with 22303 features and 2 fields
Dimension:      XY
Bounding box:  xmin: 73519.97 ymin: 6120859 xmax: 1795868 ymax: 8451928
Projected CRS: GDA2020 / MGA zone 50

Geometry type: POINT
  species      geometry
1  robusta POINT (390106.5 6462671)
2  speciosa POINT (382689.2 6457387)
3  robusta POINT (390089.8 6462603)
...
```

The GDA2020/MGA zone 50 (EPSG:7850) projection has been employed to convert the geodetic coordinates (degrees) of the *Grevillea* locations into planar coordinates (metres). For tidy data, the geographical coordinates (in the columns `lon`, `lat`) are encoded as floating point values, and are treated in the same manner as all other floating point variables. For geospatial data, they are encoded in a special data structure (in the column `geometry`) known as simple features (OGC, 2021). This simple feature encoding requires special attention since they cannot be treated like the usual floating point variables.

This paper focuses on the software implementation of the kernel smoothers, and is complementary to Chacón and Duong (2018) which focuses on the underlying statistical framework. In Section 2, we explore kernel density estimation, and in Section 3 its applications to classification (supervised learning) and density difference significance testing. In Section 4, we explore kernel density derivative estimation, and in Section 5 its applications to clustering (unsupervised learning), density ridge estimation, and modal region significance testing. In Sections 2–5, we illustrate each case first for tidy data with `ggplot2` graphics, followed by the equivalents for geospatial data with `ggplot2` and base R graphics. We outline briefly the export to external GIS software in Section 6, and kernel smoothers in other data analysis settings in Section 7. We end with some concluding remarks.

2 Density estimation

Density estimation is a fundamental statistical analysis tool, since it supplies much information about the data set at hand. Our data $\mathbf{X}_1, \dots, \mathbf{X}_n$ is a random sample drawn from the com-

mon density function f . The goal of density estimation, as its name suggests, is to estimate this unknown density. Kernel density estimates are a popular choice among the many available smoothed density estimation methods, since they posses an intuitive construction. For an arbitrary estimation point \mathbf{x} , the kernel density estimate is

$$\hat{f}_{\mathbf{H}}(\mathbf{x}) = n^{-1} \sum_{i=1}^n K_{\mathbf{H}}(\mathbf{x} - \mathbf{X}_i). \quad (1)$$

Throughout the `eks` package, the kernel function is the 2-dimensional Gaussian density function $K_{\mathbf{H}}(\mathbf{x}) = (2\pi)^{-1}|\mathbf{H}|^{-1/2} \exp(-\frac{1}{2}\mathbf{x}^\top \mathbf{H}^{-1}\mathbf{x})$. Equation (1) tells us that to compute a kernel density estimate, we place a Gaussian function, with variance \mathbf{H} , at each data point \mathbf{X}_i , and then we sum these kernel functions. This way, the data sample $\mathbf{X}_1, \dots, \mathbf{X}_n$ are transformed into a smooth surface $\hat{f}_{\mathbf{H}}$. Chacón and Duong (2018, Chapter 2) contains a more detailed overview of kernel density estimates.

The bandwidth matrix \mathbf{H} in Equation (1) is the crucial tuning parameter. A bandwidth matrix which is too small leads to an undersmoothed density estimate since it does not offer sufficient reduction in the complexity of the observed data. On the other hand, a bandwidth matrix which is too large leads to an oversmoothed density estimate that obscures important details in the observed data. Thus it is critical to find an optimal trade-off between this under- and oversmoothing. Many possible solutions for optimal smoothing are implemented in the `ks` package, and are thus available in the `eks` package, including the plug-in, unbiased cross validation and smoothed cross validation bandwidths.

2.1 Tidy density estimation

To illustrate density estimation, we focus on single species subsets of the *Grevillea* data. Figure 2 compares the density estimates for the $n = 137$ locations of the *G. leptobotrys* species which result from an optimal bandwidth from the `eks` package and from a sub-optimal one from the `ggalt` package (Rudis et al., 2017). The former, known as the bivariate plug-in bandwidth matrix (Duong and Hazelton, 2003), is the default optimal bandwidth in the `eks` package, and it is obtained from a call to `ks::Hpi`. For the *G. leptobotrys* locations, the optimal `ks::Hpi` matrix is $[2.32\text{e}8, -1.13\text{e}8; -1.13\text{e}8, 4.59\text{e}8]$. The presence of non-zero off-diagonal entries in the optimal matrix appropriately orients the kernel functions, and the resulting density estimate is unimodal, as shown in the centre panel of Figure 2. The default bandwidth in `ggalt`, which is widely used in the tidyverse, is obtained from the element-wise application of the univariate plug-in bandwidth `KernSmooth::dpik`. For the *G. leptobotrys* locations, this bandwidth is $[1.48\text{e}8, 0; 0, 1.87\text{e}8]$. Since this sub-optimal matrix only applies smoothing in the coordinate axis directions, it yields an undersmoothed density estimate with spurious multi-modal structure on the right panel.

In Figure 2, the heights of the contour regions are calculated according to the probability contours method (Bowman and Foster, 1993, Hyndman, 1996). The pink region is the smallest region that contains 25% of the probability mass, the orange region plus the enclosed pink region is the smallest region that contains 50% of the probability mass, and the yellow region plus the enclosed orange and pink regions is the smallest region that contains 75% of the probability mass. Since these are relative heights, they facilitate the choice of the contour levels, since it involves selecting values from 0% to 100%, rather than from the range of the density values. These probability contours can also be considered as a multivariate extension of the univariate percentiles, e.g., the 50% contour region is a bivariate equivalent to the median. Due to

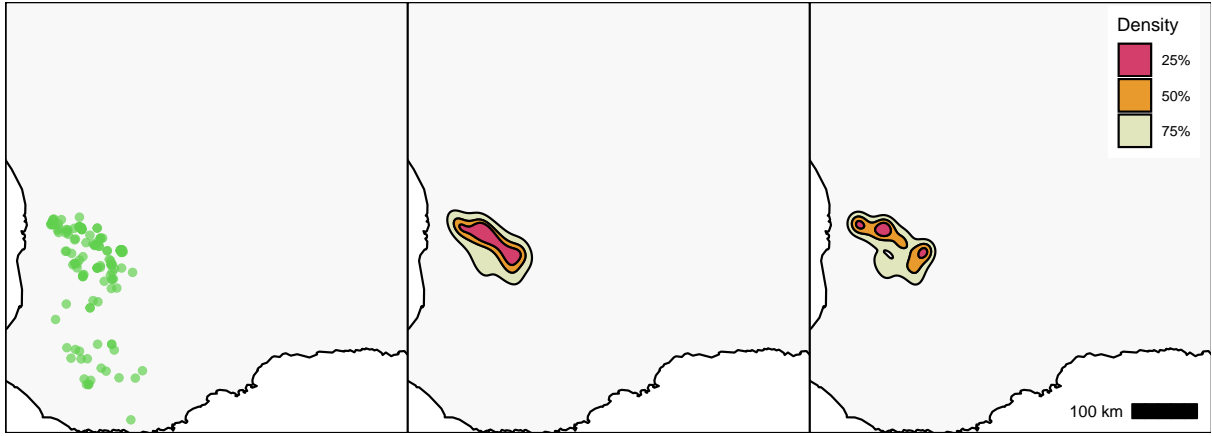


Figure 2: Filled contour plots of density estimates for *G. leptobotrys* ($n = 137$) with quartile probability contour levels. (Left) Scatter plot. (Centre) Optimally smoothed. (Right) Under-smoothed.

their intuitive properties, these probability contours are employed throughout in `eks`, with the quartile contour levels (25%, 50%, 75%) being the default values. In addition to their intuitive interpretation, these probability contours are straightforward to compute: the kernel density estimate is evaluated at the n observed data values $\hat{f}_{\mathbf{H}}(\mathbf{X}_1), \dots, \hat{f}_{\mathbf{H}}(\mathbf{X}_n)$, then we compute τ_α as the α -quantile of these evaluated values, and the α probability contour region is the level set of the density estimate at τ_α , i.e. $\{\mathbf{x} : \hat{f}_{\mathbf{H}}(\mathbf{x}) > \tau_\alpha\}$ (Hyndman, 1996).

In contrast to *G. leptobotrys*, for the $n = 93$ locations of the *G. yorkrakinensis* species, the optimally smoothed density estimate in the centre panel in Figure 3 displays a trimodal structure with obliquely oriented contours. The oversmoothed density estimate in the right panel has circular contours and a bimodal structure, and is unable to distinguish between the two modal regions in the lower right. The optimal bandwidth matrix is $[8.84\text{e}8, -8.33\text{e}8; -8.33\text{e}8, 1.36\text{e}9]$, whereas the sub-optimal bandwidth is $[5.43\text{e}8, 0; 0, 9.10\text{e}8]$. If we take Figures 2–3 together, optimal smoothing prevents both under- and oversmoothing.

The R code snippets included here are intended to give an overall idea of the syntax of the `eks` package, rather than a complete code to reproduce the figures. The latter is provided in the companion R script (`eks-script.R`). This first code snippet treats the *G. yorkrakinensis* data as a tidy data set (`yorkr_coord`). The commands to compute the density estimate with the optimal bandwidth, in the centre panel in Figure 2, are

```
R> ## tidy density estimate
R> yorkr_coord <- dplyr::filter(grevilleasf_coord, species=="yorkrakinensis")
R> yorkr_coord <- dplyr::select(yorkr_coord, lon, lat)
R> t1 <- tidy_kde(yorkr_coord)
R> ggplot2::ggplot(t1, ggplot2::aes(x=lon, y=lat)) +
+   geom_contour_filled_ks(colour=1)
```

The function `tidy_kde` is a wrapper function for `ks::kde`. It computes the tidy density estimate explicitly. This differs from existing layer functions, e.g., `ggplot2::geom_density_2d` and `ggalt::geom_bkde2d`, which compute the density estimate internally and do not return a user-level R object. The tidy density estimate output from `tidy_kde` is:

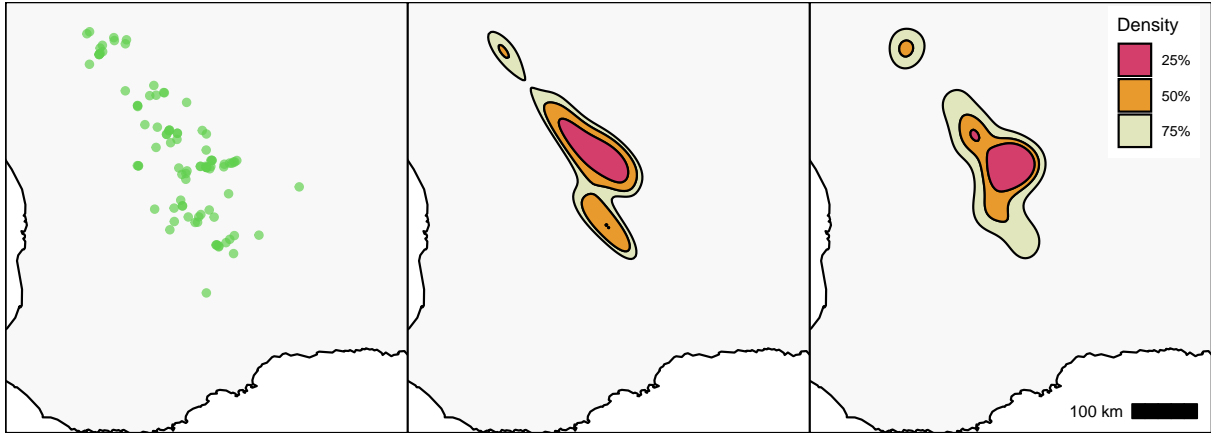


Figure 3: Filled contour plots of density estimates for *G. yorkrakinensis* ($n = 93$) with quartile probability contour levels. (Left) Scatter plot. (Centre) Optimally smoothed. (Right) Over-smoothed.

```
R> t1
# A tibble: 22,801 × 6
  lon      lat estimate ks      tks      label
  <dbl>    <dbl>    <dbl> <list>    <chr> <chr>
1 378915. 6207697.     0 <kde>    kde  Density
2 382385. 6207697.     0 <int [1]> kde  Density
3 385855. 6207697.     0 <int [1]> kde  Density
...
...
```

The output is a tibble with an added `tidy_ks` class. This allows for a `ggplot.tidy_ks` method to be defined for this object class. Otherwise, it can be treated as a tibble. The first two columns `lon`, `lat` (same names as the input data) are the coordinates of the vertices in the estimation grid, the third column `estimate` is the density estimate value at `lon`, `lat`. The fourth column `ks` holds the output from `ks::kde`. This is required for the computation of probability contours in the new layer function `geom_contour_filled_ks` which draws the filled contour plots for `tidy_ks` objects. The remaining columns indicate that the output is a density estimate computed from `ks::kde`, and they are employed in `ggplot.tidy_ks` to create default aesthetic mapping and legend labels. This default aesthetic mapping is `ggplot2::aes(x=lon, y=lat, z=estimate, weight=ks)`. Whilst the `x`, `y`, `z` aesthetics are as expected for a bivariate contour plot, the `weight` aesthetic is unorthodox, since it is not a weighting variable: it is a workaround in `ggplot2` graphics to mimic the dynamic display of probability contours in base R graphics.

For the *G. yorkrakinensis* data, the quartile contour levels for the optimally smoothed density estimate in the centre panel in Figure 3 are 1.81e-11, 2.23e-11, 2.91e-11, and for the under-smoothed density estimate in the right panel are 1.63e-11, 2.29e-11, 2.75e-11. These probability contour heights are different for each different density estimate, even if the target contour probabilities remain the same. On the other hand, it is sometimes useful to have a set of fixed contour heights for all density estimates for a direct comparison. Computing a suitable set of contour heights most likely needs some trial and error to produce visually appealing contour plots for all density estimates (Chacón and Duong, 2018, Section 2.2). A heuristic solution

consists of computing the probability contour heights for each density estimate, for a fixed set of probabilities, which are then aggregated. We compute the corresponding probabilities for each density estimate for this aggregated set of contour heights, and we remove any contour levels whose estimated probability which are too close to each other. This procedure is implemented in `contour_breaks`, and whose output can be then input into `geom_contour_filled_ks` by setting the `breaks` parameter.

We revisit the density estimates for the *G. yorkrakinensis* locations, this time with the fixed contour heights (9.25e-12, 1.85e-11, 2.46e-11, 4.01e-11). With these fixed contour heights, a direct comparison of different density estimates is possible. The density estimate on the right exceeds the highest density value (4.01e-11, dark pink), whereas the optimally smoothed estimate only exceeds the second highest value (2.46e-11, dark orange). Since the former misses some important modal information, then it is indeed oversmoothed in comparison.

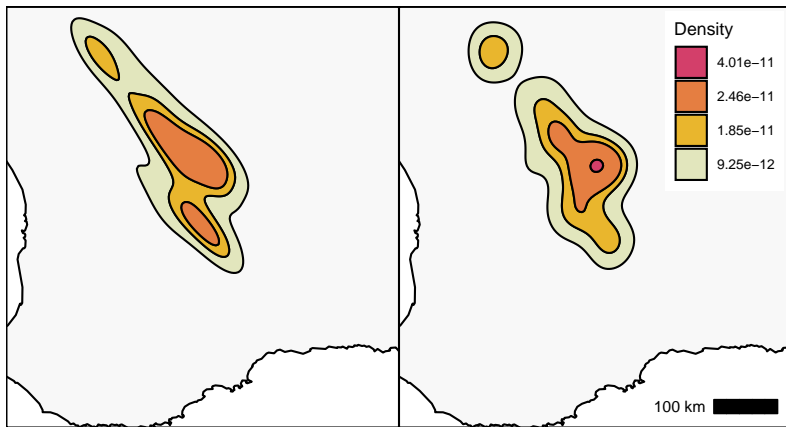


Figure 4: Filled contour plots of density estimates for *G. yorkrakinensis* ($n = 93$) with fixed contour levels. (Left) Optimally smoothed. (Right) Oversmoothed.

The code to produce two density estimates with a single set of contour heights in Figure 4 is

```
R> ## fixed contour levels
R> H2 <- diag(sapply(yorkr_coord, KernSmooth:::dpik)^2)
R> t2 <- tidy_kde(yorkr_coord, H=H2)
R> t3 <- c(t1, t2)
R> b <- contour_breaks(t3, cont=c(10,30,50,70,90))
R> ggplot2::ggplot(t3, ggplot2::aes(x=lon, y=lat)) +
+   geom_contour_filled_ks(colour=1, breaks=b) + ggplot2::facet_wrap(~group)
```

To emphasise that the `eks` package is equally capable of computing a kernel density estimate for tidy data which are not also geospatial coordinates (as is the case for `grevilleasf_coord`), we examine the well-known `crabs` data set from the `MASS` package:

```
R> crabs
  sp sex index   FL   RW   CL   CW   BD
1  B   M      1 8.1 6.7 16.1 19.0 7.0
2  B   M      2 8.8 7.7 18.1 20.8 7.4
3  B   M      3 9.2 7.8 19.0 22.4 7.7
...
...
```

This data set consists of $n = 200$ observations for 50 crabs, each of two colour forms and two sexes, of the species *Leptograpsus variegatus* collected in Western Australia. We focus on the frontal lobe size FL (mm) and carapace width CW (mm) measurements. The effect of oversmoothing, with the default bandwidths $[2.23, 0; 0, 9.50]$, on the right panel of Figure 5 is even more apparent than in Figure 4. The bimodality of the optimally smoothed density estimate with bandwidths $[1.45, 3.47; 3.47, 8.38]$ is highly detailed, whereas it is completely absent for the oversmoothed estimate.

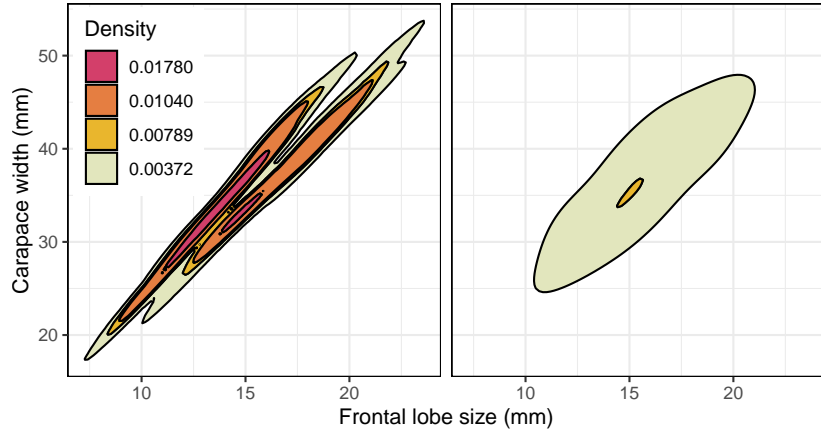


Figure 5: Filled contour plots of density estimates for *L. variegatus* crabs ($n = 200$) with fixed contour levels. (Left) Optimally smoothed. (Right) Oversmoothed.

For brevity, we do not display any more figures for these `crabs` data when demonstrating tidy kernel methods in the sequel, since they would be conceptually identical to those for the *Grevillea* data.

2.2 Geospatial density estimation

To produce a map like in the centre panel in Figure 3 for the *G. yorkrakinensis* locations as geospatial data (`yorkr`), the commands are

```
R> ## geospatial density estimate
R> yorkr <- dplyr::filter(grevilleasf, species=="yorkrakinensis")
R> s1 <- st_kde(yorkr)
```

The function `st_kde` is the geospatial equivalent of `tidy_kde`, and produces an object of class `sf_ks`, which is a list of 3 fields: `tidy_ks`, `grid`, and `sf`. The first field is a summary of the tidy density estimate from `tidy_kde`, the second are the rectangular polygons of the estimation grid, and the third are the 1% to 99% probability contour regions of the density estimate. We focus on the contour regions.

```
R> s1$sf
Simple feature collection with 99 features and 2 fields
Geometry type: MULTIPOLYGON
  contlabel      estimate           geometry
1       99 3.469482e-12 MULTIPOLYGON (((366008.4 64...
2       98 4.373744e-12 MULTIPOLYGON (((368748.9 64...
```

```
3      97 5.781100e-12 MULTIPOLYGON (((374230.1 64...
```

```
...
```

This has 2 attributes: `contlabel` (label for the probability contour) and `estimate` (height of contour probability region). Unlike for `tidy_kde` where the probability contour regions are computed dynamically in the layer function `geom_contour_filled_ks`, these 1% to 99% regions are converted to multipolygons prior to plotting since the dynamic conversion during plotting could be computationally heavy. The quartile contours 25%, 50%, 75% are selected by default in `geom_contour_filled_ks` for tidy data. Since we are unable replicate exactly this automatic behaviour for the `ggplot2::geom_sf` layer function, we first apply `st_get_contour` to the input of `ggplot2::geom_sf`. The `sf_ks` class also has a `ggplot.sf_ks` method which computes the default map legend.

```
R> ## geospatial density estimate geom_sf plot
R> ggplot2::ggplot(s1) + ggplot2::geom_sf(data=st_get_contour(s1),
+ ggplot2::aes(fill=contlabel))
```

The display of geospatial data is more flexible than that for tidy data since the former can be displayed in either the `ggplot2` or base R graphics without any change to the input. The density estimate output from `st_kde` is displayed in base R graphics via the `plot.sf_ks` method for `sf_ks` objects. The following command produces the equivalent output to the centre panel in Figure 3.

```
R> ## geospatial density estimate base R plot
R> plot(s1)
```

This plot method internally calls `st_get_contour` to extract the required contour polygons for plotting, so it is more concise than `ggplot2::geom_sf` that requires an explicit user-level call to `st_get_contour`. The base R and `ggplot2` plots are essentially identical since they comply with the geospatial standard specifications (OGC, 2021).

2.3 Optimal bandwidth matrices

Since the bandwidth matrix is the crucial tuning parameter for kernel density estimates, we explore further their statistical properties. These properties are the subject of a vast body of research literature, which we do not attempt to review here, and instead provide a simplified outline of how the optimal bandwidth matrix in `eks` is obtained.

We begin with a squared error discrepancy between a density estimate $\hat{f}_{\mathbf{H}}$ and the target density f , i.e., $M(\mathbf{H}) = \int \mathbb{E}[\hat{f}_{\mathbf{H}}(\mathbf{x}) - f(\mathbf{x})]^2 d\mathbf{x}$. Since this expression involves the unknown target density f , it must be estimated for it to be of practical use. The plug-in bandwidth matrix in `ks:::Hpi` computes the estimate $\hat{M}(\mathbf{H}) = (4\pi)^{-d/2} n^{-1} |\mathbf{H}|^{-1/2} + \frac{1}{4} \hat{\mathbf{m}}_4^\top (\text{vec } \mathbf{H} \otimes \text{vec } \mathbf{H})$. We omit to describe this estimate rigorously since it would require lengthy technical definitions: the interested reader is encouraged to consult Chacón and Duong (2018, Chapter 3) for details. We are content to state that the first term in \hat{M} is related to the variance of the density estimate, and the second term to the square of the bias of the density estimate. An optimal bandwidth matrix $\hat{\mathbf{H}}$ is defined as

$$\hat{\mathbf{H}} = \underset{\mathbf{H}}{\text{argmin}} \hat{M}(\mathbf{H}) \quad (2)$$

where the minimisation is carried out over the space of all symmetric positive definite matrices. When this minimisation is achieved, then there is an optimal trade-off between the variance

and the squared bias, or equivalently between under- and over-smoothing. When an optimal bandwidth matrix $\hat{\mathbf{H}}$ is substituted into Equation (1), the resulting kernel density estimate is the closest to the target density f as measured by the discrepancy \hat{M} . Different bandwidth matrices arise from the different ways of computing \hat{M} and/or from different ways of carrying out the minimisation. For example, the default bandwidth in `ggalt` treats the joint bivariate optimisation in Equation (2) as two separate univariate optimisation problems. The density estimate functions `tidy_kde` and `st_kde` compute $\hat{\mathbf{H}}$ in Equation (2) by calling the `ks::Hpi` function, and then substitute this $\hat{\mathbf{H}}$ into Equation (1), to compute an optimal tidy/geospatial density estimate, as shown in the centre panels in Figures 2–3.

Additional bandwidth matrices in the `ks` package include the normal scale `ks::Hns`, unbiased cross validation `ks::Hucv` and smoothed cross validation `ks::Hscv`. The commands are of the type:

```
R> ## smoothed cross validation selector
R> H3 <- ks::Hscv(yorkr_coord)
R> t3 <- tidy_kde(yorkr_coord, H=H3)
```

For most data samples, the plug-in bandwidth `ks::Hpi` yields fast and robust kernel estimates, though there remain some cases where other bandwidths are more suitable. For a review of the performance of these other bandwidths, see Chacón and Duong (2018, Chapter 3). For brevity, we illustrate kernel estimates only with the plug-in optimal bandwidths in the sequel.

3 Applications of density estimates

For tidy and geospatial data, kernel smoothing methodologies other than stand-alone density estimates are rarely implemented. We demonstrate the increased scope of kernel smoothers in the `eks` package with some applications of density estimates to density-based classification (supervised learning) and to significant density difference testing.

3.1 Density-based classification (supervised learning)

The goal of classification is to assign future data to one of the known classes in the current data. That is, this is a supervised learning problem. The data are $(\mathbf{X}_1, Y_1), \dots, (\mathbf{X}_n, Y_n)$, where the \mathbf{X}_i are the observed attributes, and the Y_i is the known class label from m classes. These data are a random sample from the mixture density $\pi_1 f_1 + \dots + \pi_m f_m$, where π_j is the prior probability and f_j is the marginal density function for class j , for $j = 1, \dots, m$ (Chacón and Duong, 2018, Section 7.2).

The simplest (and often most robust) classifier is the Bayes classifier. This assigns a candidate point \mathbf{x} to the class c with the highest density value at \mathbf{x} , i.e., $c(\mathbf{x}) = \operatorname{argmax}_{j=1, \dots, m} \pi_j f_j(\mathbf{x})$. The density-based classifier replaces the prior probability π_j with the observed sample class proportion $\hat{\pi}_j$, and the marginal density f_j with the marginal density estimate \hat{f}_j . Each marginal density estimate is computed with its own optimal bandwidth matrix. The estimated class label for \mathbf{x} from the kernel density-based classifier is thus

$$\hat{c}(\mathbf{x}) = \operatorname{argmax}_{j=1, \dots, m} \hat{\pi}_j \hat{f}_j(\mathbf{x}).$$

This kernel classifier is more adaptable than the usual linear and quadratic classifiers. The linear classifier uses Gaussian density fits with a common variance matrix for all classes, and the quadratic classifier Gaussian density fits with a different variance matrix for each class.

Our data sample comprises the combined *G. hakeoides* (pink circles, $n_1 = 207$) and *G. paradoxa* (green triangles, $n_2 = 358$) data samples, as shown in the scatter plot in the left panel of Figure 6. In the centre panel are the quartile probability contour plots of marginal density estimates $\hat{\pi}_1 \hat{f}_1$ (pink lines) and $\hat{\pi}_2 \hat{f}_2$ (green lines), where \hat{f}_1 is the density estimate for *G. hakeoides*, and \hat{f}_2 for *G. paradoxa*. As the marginal density contours have considerable overlap in the central modal region, it is difficult to decide visually which marginal density value is higher. This is resolved in the plot of estimated class labels from the density-based classifier on the right of Figure 6. The regions where *G. hakeoides* is more likely are coloured in pink, and where *G. paradoxa* is more likely are in green.

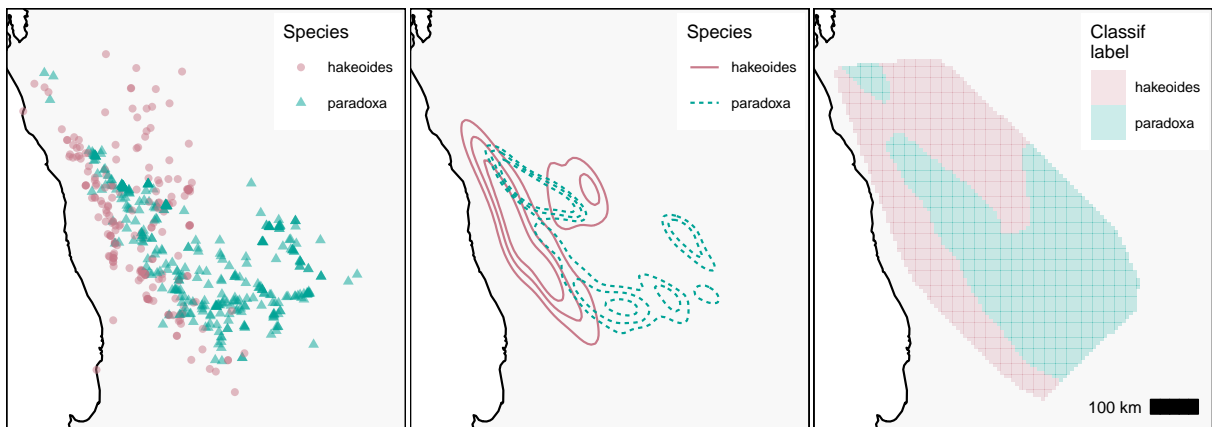


Figure 6: Density-based classifier for *G. hakeoides* ($n_1 = 207$) and *G. paradoxa* ($n_2 = 358$). (Left) Scatter plots. (Centre). Quartile probability contours of marginal density estimates. (Right) Class label estimates.

The command to compute a tidy kernel classifier is `tidy_kda`. It requires a grouped tibble as its input (`grevilleasf_gr_coord`), grouped by the class factor variable (`species`). To produce the marginal densities plot for the density-based classifier in the centre panel in Figure 6:

```
R> ## tidy density-based classifier contours
R> t4 <- tidy_kda(grevilleasf_gr_coord)
R> ggplot2::ggplot(t4, ggplot2::aes(x=lon, y=lat)) +
+   geom_contour_ks(ggplot2::aes(colour=species))
```

The layer function `geom_contour_ks` draws the contour lines for `tidy_ks` objects. In addition to the columns already present in the density estimate, the extra columns in the output of a density-based classifier relate to the classes: `prior_prob` (class sample proportion), `label` (estimated class label), `species` (same as input class label). The structure of a density-based classifier is similar to that for a density estimate grouped by a class variable.

Moreover, we do not wish to plot the default rectangular display grid as this contains labels for pixels in the ocean. So prior to the generating the display using `ggplot2::geom_tile` in the right panel in Figure 6, we compute the estimates of the density support via `tidy_ksupp`, and assign an `NA` class label to those pixels outside of the convex hull of the union of the density support estimates.

```
R> ## tidy density-based classifier labels plot
```

```
R> ggplot2::ggplot(t4, ggplot2::aes(x=lon, y=lat)) +
  ggplot2::geom_tile(ggplot2::aes(fill=label), alpha=0.1)
```

The equivalent code to produce a geospatial density-based classifier is

```
R> ## geospatial density-based classifier
R> s4 <- st_kda(grevilleasf_gr)
```

where `grevilleasf_gr` is the geospatial version of `grevilleasf_gr_coord`. The estimated class labels are stored in the `sf_ks` object in the `grid` field as a collection of rectangular polygons. To plot these class labels, for a `ggplot2` plot, we call `ggplot2::geom_sf` on the `grid` field, and for a base R plot, we call `plot(, which_geometry=="grid")`.

```
R> ## geospatial density-based classifier geom_sf plot
R> gs <- ggplot2::ggplot(s4)
R> gs + ggplot2::geom_sf(data=s4$grid, ggplot2::aes(fill=label), alpha=0.2,
+ colour=NA)
R> gs + ggplot2::geom_sf(data=st_get_contour(s4),
+ ggplot2::aes(colour=species), fill=NA)
R> ## base R plot
R> plot(s4, which_geometry="grid", border=NA)
R> plot(s4, which_geometry="sf")
```

The question of optimal bandwidths for a density-based classifier is more complicated than that for a density estimate. We opt for a simple and robust implementation in the `eks` package, where `tidy_kda` and `st_kda` call `ks::Hpi` for each class data sub-sample. These class-wise optimal bandwidths are known to asymptotically minimise the misclassification error, i.e., the probability that we do not classify a candidate point in class j given that it is drawn from class j , $\mathbb{P}\{\hat{c}(\mathbf{X}) \neq j | \mathbf{X} \sim f_j\}$. Whilst there is an intuitive appeal in selecting bandwidths to exactly minimise the misclassification error, it is not clear how much is gained in practise with this more complicated approach over the simpler bandwidths. Moreover, there are currently no efficient computational algorithms to compute these more complicated bandwidths. See Chacón and Duong (2018, Section 7.2) for a discussion.

3.2 Local density difference hypothesis testing

We make our first foray into kernel-based statistical inference. The goal is to determine the regions where two density functions are statistically significantly different from each other. Whilst hypothesis tests for global differences are well-known, e.g., Kolmogorov-Smirnov, these do not indicate where in the data the differences are most salient. Towards this goal, we employ local hypothesis tests based on the difference of the density functions. For each candidate point \mathbf{x} , the local null hypothesis is $H_0(\mathbf{x})$: $f_1(\mathbf{x}) = f_2(\mathbf{x})$. From these local hypothesis tests, we define the significant density difference regions as

$$U^+ = \{\mathbf{x} : \text{reject } H_0(\mathbf{x}), f_1(\mathbf{x}) > f_2(\mathbf{x})\}, \quad U^- = \{\mathbf{x} : \text{reject } H_0(\mathbf{x}), f_1(\mathbf{x}) \leq f_2(\mathbf{x})\}.$$

The data $\mathbf{X}_1, \dots, \mathbf{X}_{n_1}$ is an n_1 random sample drawn from the first density function f_1 , and $\mathbf{Y}_1, \dots, \mathbf{Y}_{n_2}$ an n_2 sample from the second density function f_2 . The local test statistic, as proposed in Duong (2013), is $W(\mathbf{x}) = [\hat{f}_1(\mathbf{x}) - \hat{f}_2(\mathbf{x})]^2 / S(\mathbf{x})^2$, where $S(\mathbf{x})^2$ is an estimate of the

variance of $\hat{f}_1(\mathbf{x}) - \hat{f}_2(\mathbf{x})$. This author computes an expression for $S(\mathbf{x})^2$, and establishes that the null distribution of the test statistic $W(\mathbf{x})$ is asymptotically chi-squared with 1 d.f. for all candidate points \mathbf{x} . See also Chacón and Duong (2018, Section 7.1).

We carry out these hypothesis tests $H_0(\mathbf{x}_j), j = 1, \dots, m$ for all the candidate points in a grid $\{\mathbf{x}_1, \dots, \mathbf{x}_m\}$. Let the p -value from $H_0(\mathbf{x}_j)$ at significance level α be $p_j = \mathbb{P}(W(\mathbf{x}_j) > \chi_1^2(1-\alpha))$. Let the order statistics of these p -values be $p_{(1)} \leq \dots \leq p_{(m)}$, and their corresponding hypotheses $H_{0,(1)}, \dots, H_{0,(m)}$. The Hochberg decision rule rejects all the hypotheses $H_{0,(1)}, \dots, H_{0,(j^*)}$ where $j^* = \text{argmax}_{1 \leq j \leq m} \{p_{(j)} \leq \alpha/(m - j + 1)\}$. This rule controls the Type 1 error (false positive) to the level of significance α across all these tests (Hochberg, 1988).

Now that we are able to determine for which candidate points \mathbf{x}_j we reject the local hypothesis tests, then the estimates of the significant density difference regions are

$$\begin{aligned}\hat{U}^+ &= \{\mathbf{x}_j : \text{reject } H_0(\mathbf{x}_j) \text{ and } \hat{f}_1(\mathbf{x}_j) > \hat{f}_2(\mathbf{x}_j), j = 1, \dots, m\} \\ \hat{U}^- &= \{\mathbf{x}_j : \text{reject } H_0(\mathbf{x}_j) \text{ and } \hat{f}_1(\mathbf{x}_j) \leq \hat{f}_2(\mathbf{x}_j), j = 1, \dots, m\}.\end{aligned}$$

The local density difference hypothesis testing procedure is implemented in `tidy_local_test` and `st_local_test`. The results for testing between $n_1 = 207$ *G. hakeoides* and $n_2 = 358$ *G. paradoxa* locations at an $\alpha = 0.05$ level of significance are displayed in Figure 7. The regions where *G. hakeoides* is significantly more prevalent are in pink, and where *G. paradoxa* is significantly more prevalent are in green. These significant density difference regions are superposed on the density-based classifier labels from Figure 6, reproduced here as the pale pink and pale green regions. The density-based classifier always assigns one of these classes (species) to all points, even in the borderline cases where both density estimates are of similar value, and/or where the data are sparse. The significant density difference region estimates, due to a more stringent threshold of statistical evidence, do not include these borderline cases. Hence they yield more targeted regions of relative prevalence.

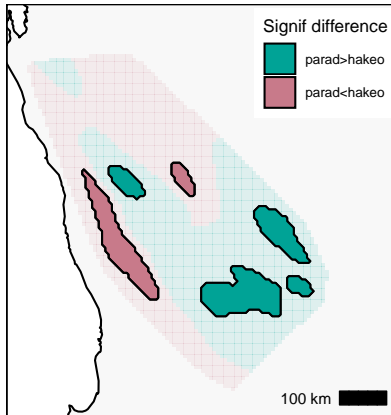


Figure 7: Local significant density difference region estimates ($\alpha = 0.05$) for *G. hakeoides* ($n_1 = 207$) and *G. paradoxa* ($n_2 = 358$), superposed on the density-based classifier regions. Regions where *G. hakeoides* is statistically more prevalent are in pink, and where *G. paradoxa* is more prevalent are in green. Density-based classifier regions are pale pink for *G. hakeoides*, and pale green for *G. paradoxa*.

The commands for these local density difference hypothesis tests are `tidy_kde_local_test` and `st_kde_local_test`. These local tests require two separate input data sets, which are

`parad_coord`, `hakeo_coord` (tidy) and `parad`, `hakeo` (geospatial) for the *G. hakeoides* and *G. paradoxa* data samples.

```
R> ## tidy signif. density difference regions
R> t6 <- tidy_kde_local_test(data1=parad_coord, data2=hakeo_coord)
R> ggplot2::ggplot(t6, ggplot2::aes(x=lon, y=lat)) +
+   geom_contour_filled_ks(colour=1)

R> ## geospatial signif. density difference regions geom_sf plot
R> s6 <- st_kde_local_test(x1=parad, x2=hakeo)
R> ggplot2::ggplot(s6) +
+   ggplot2::geom_sf(data=st_get_contour(s6), ggplot2::aes(fill=label))
R> ## base R plot
R> plot(s6)
```

The output is similar to that for a single density estimate, except that the density value at `(lon, lat)` is replaced by an indicator of which data sample is significantly more prevalent `(label)`. Hence the plotting behaviour is similar to that for a density estimate.

The question of optimal bandwidths for a significant density difference region estimate is analogous to that for a density-based classifier, and we opt for a similar solution where `tidy_kde_local_test` and `st_kde_local_test` call `ks::Hpi` for each class data sample. These sample-wise plug-in bandwidths most likely asymptotically minimise the symmetric difference between \hat{U}^+ and U^+ , and between \hat{U}^- and U^- , though it has not yet been shown rigorously. Nonetheless empirical evidence indicates that these plug-in bandwidths offer effective estimates of the significant density difference regions.

4 Density derivative estimation

Crucial information about the structure of a data set is not always revealed by examining solely the density values, and can only be discerned via the density derivatives. For example, the local maxima of the data density are characterised as the locations where the first derivative is the identically zero and the second derivative is negative definite (Chacón and Duong, 2018, Chapter 5). Some recent examples of the utility of density derivative estimates in data analysis include: the segmentation of digital images, which utilised the first density derivative of pixel colour-locations to guide the search for similar image segments more efficiently than using only the density of the pixel colour-locations (Beck et al., 2016); and the identification of differences in cell fluorescence measurements between healthy control and diseased subjects (Chacón et al., 2011), which utilised the second density derivative to pinpoint more robustly the biologically different regions than is possible by considering only the density of the fluorescence measurements.

With the same data as for the density estimation case, i.e., $\mathbf{X}_1, \dots, \mathbf{X}_n$ is a random sample drawn from the common density function f , our goal is to estimate the derivatives of the unknown density f , focusing on the first (gradient) derivative. For 2-dimensional data, the gradient of a density function f is comprised of two partial derivatives $\mathbf{D}f = [\partial f / \partial x_1, \partial f / \partial x_2]$. The kernel estimate of the density gradient is given by

$$\mathbf{D}\hat{f}_{\mathbf{H}}(\mathbf{x}) = n^{-1} \sum_{i=1}^n \mathbf{D}K_{\mathbf{H}}(\mathbf{x} - \mathbf{X}_i) \quad (3)$$

where the gradient kernel function is $DK_{\mathbf{H}}(\mathbf{x}) = -(2\pi)^{-1}|\mathbf{H}|^{-1/2}\mathbf{H}^{-1}\mathbf{x}\exp(-\frac{1}{2}\mathbf{x}^\top\mathbf{H}^{-1}\mathbf{x})$. Since there are two components of the density gradient, it can be visualised using two separate plots, one for each partial derivative. A more concise alternative is a quiver plot, in which arrows, whose length and direction are determined by the gradient, are drawn at each point in the estimation grid. Figure 8 is the quiver plot for the density gradient estimate for *G. yorkrakinensis*, superposed on the density estimate. The arrows for the density gradient point towards the peaks of the modal regions. These arrows are longer where the density gradient is steeper, and they are shorter in the density tails where the slope is flatter. These density gradients indicate the rate of change in the data density, which is not easy to ascertain from the density levels themselves in the underlying density contour plot.

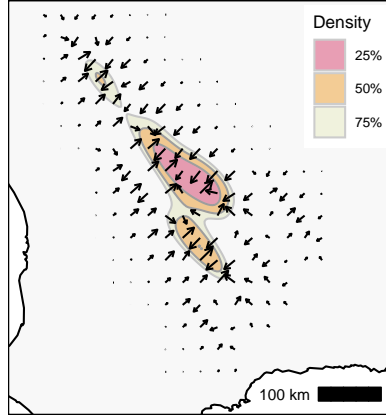


Figure 8: Quiver plot of density gradient estimate for *G. yorkrakinensis* ($n = 93$), superposed over its density estimate.

The command for a tidy density gradient estimate is `tidy_kdde(, deriv_order=1)`. The function `tidy_kquiver` converts the output from `tidy_kdde` into a format suitable for the quiver plot layer function `ggquiver::geom_quiver` (O'Hara-Wild, 2019). For *G. yorkrakinensis*, the code to produce a quiver plot superposed on a density estimate is

```
R> ## tidy density gradient estimate plot
R> t7 <- tidy_kdde(yorkr_coord, deriv_order=1)
R> t8 <- tidy_kquiver(t7)
R> ggplot2::ggplot(t1, ggplot2::aes(x=lon, y=lat)) +
+   ggquiver::geom_quiver(data=t8, ggplot2::aes(u=u, v=v))
```

The output from `tidy_kdde` is a tibble which is grouped by `deriv_group`. The columns present in a density estimate are also present in a density derivative estimate, along with some additional columns relating to the derivative: `deriv_order` (derivative order, 1 for the gradient), `deriv_ind` (partial derivative enumeration, from 1 to 2), `deriv_group` (partial derivative indices (1,0), (0,1) which correspond to $\partial/\partial x_1, \partial/\partial x_2$ respectively).

Whilst with `st_kquiver` we can compute a geospatial output, `ggplot2::geom_sf` is not able to plot arrows, and it is not possible to overlay a `ggquiver::geom_quiver` layer over a `geom_sf` layer. The current work-around is to overlay a `ggplot2::geom_segment` layer over a `geom_sf` layer, with some trial and error required in `grid::arrow` to produce suitable arrows.

```
R> ## geospatial density gradient estimate geom_sf plot
```

```
R> s7 <- st_kdde(yorkr, deriv_order=1)
R> s8 <- st_kquiver(s7, thin=9)
R> ggplot2::ggplot(s1) + ggplot2::geom_segment(data=s8$sf,
+ ggplot2::aes(x=lon, xend=lon_end, y=lat, yend=lat_end),
+ arrow=grid::arrow(length=0.1*s8$sf$len))
```

On the other hand, for a base R plot, the display of geospatial and tidy data are freely interchangeable, so we can overlay the quiver plot `plot(, display="quiver")` for a kernel density gradient estimate from the `ks` package.

```
R> ## geospatial density gradient estimate base R plot
R> plot(s8$tidy_ks$ks[[1]], display="quiver")
```

For optimal bandwidth selection for kernel density gradient estimates, it is crucial to note that the optimal bandwidth matrix for $D\hat{f}_{\mathbf{H}}$ is not the same as that for $\hat{f}_{\mathbf{H}}$. For a density estimate the optimality criterion is $M(\mathbf{H}) = \int \mathbb{E}[\hat{f}_{\mathbf{H}}(\mathbf{x}) - f(\mathbf{x})]^2 d\mathbf{x}$, whereas the criterion for a density gradient estimate is $M_1(\mathbf{H}) = \int \mathbb{E}\|D\hat{f}_{\mathbf{H}}(\mathbf{x}) - Df(\mathbf{x})\|^2 d\mathbf{x}$. Since $M \neq M_1$ then their minimisers will also not be equal in general. The default optimal bandwidth for the density gradient estimate in the `eks` package is the plug-in bandwidth (Chacón and Duong, 2010) obtained from a call to `ks::Hpi(, deriv.order=1)`. For the *G. yorkrakinensis* data, this bandwidth matrix is $[4.39e8, -4.36e8; -4.36e8, 7.73e8]$. In comparison, the optimal bandwidth matrix for the density estimate is $[8.84e8, -8.33e8; -8.33e8, 1.36e9]$. See Chacón and Duong (2018, Section 5.7) for more details.

Whilst `eks` provides functionality for the computation and display of the kernel estimates of Hessian (second) derivative of the density, we omit them since there does not exist currently a suitably compelling visualisation like the quiver plot. However density Hessian estimates are a key element in other data analysis applications.

5 Applications of density derivative estimates

The true added value of density derivative estimates are as key components in more complex data analysis applications. We demonstrate the crucial role that density gradient estimates play in density-based clustering, and that density Hessian estimates play in density ridge estimates and significant density curvature regions.

5.1 Density-based clustering (unsupervised learning)

The goal of clustering is to discover homogeneous groups within a data set in a trade-off between similarity/dissimilarity: members of the same cluster are similar to each other while members of different clusters are dissimilar to each other. If the q unknown population clusters are $\{C_1, \dots, C_q\}$, then the cluster labelling function is $c(\mathbf{x}) = j$ whenever a candidate point \mathbf{x} belongs to cluster C_j . Whilst we are able to estimate the cluster labelling function for all candidate points, for the vast majority of data analysis cases, it is sufficient to compute $\hat{c}(\mathbf{X}_1), \dots, \hat{c}(\mathbf{X}_n)$ for the data sample $\mathbf{X}_1, \dots, \mathbf{X}_n$. Since the cluster labels are unknown, then this is an unsupervised learning problem.

Many clustering algorithms have been proposed in the literature. Our chosen approach is density-based clustering, where a cluster is a data-rich region (high density values) which is separated from another data-rich region by a data-poor region (low density values). Thus we

associate each data point to its ‘most representative’ data-rich region. In the `eks` package, this is carried out with a mean shift algorithm (Fukunaga and Hostetler, 1975). For a data point \mathbf{X}_i , we initialise a sequence with $\mathbf{X}_{i,0} = \mathbf{X}_i$, then we iterate the recurrence equation

$$\mathbf{X}_{i,k+1} = \mathbf{X}_{i,k} + \mathbf{H}^{-1} \mathbf{D}\hat{f}_{\mathbf{H}}(\mathbf{X}_k) / \hat{f}_{\mathbf{H}}(\mathbf{X}_k),$$

where $\hat{f}_{\mathbf{H}}$ is a density estimate and $\mathbf{D}\hat{f}_{\mathbf{H}}$ is a density gradient estimate. This recurrence equation is closely related to the well-known gradient ascent algorithm, with the improvement that accelerates the convergence of the recurrence iterations in regions of low data density. A more computationally stable form of the mean shift recurrence equation is

$$\mathbf{X}_{i,k+1} = \mathbf{X}_{i,k} + \boldsymbol{\beta}_{\mathbf{H}}(\mathbf{X}_{i,k}) = \frac{\sum_{\ell=1}^n \mathbf{X}_{\ell} g((\mathbf{X}_{i,k} - \mathbf{X}_{\ell})^{\top} \mathbf{H}^{-1} (\mathbf{X}_{i,k} - \mathbf{X}_{\ell}))}{\sum_{\ell=1}^n g((\mathbf{X}_{i,k} - \mathbf{X}_{\ell})^{\top} \mathbf{H}^{-1} (\mathbf{X}_{i,k} - \mathbf{X}_{\ell}))} \quad (4)$$

where $g(x) = x \exp(-\frac{1}{2}x)$ and $\boldsymbol{\beta}_{\mathbf{H}}(\mathbf{x}) = \frac{\sum_{\ell=1}^n \mathbf{X}_{\ell} g((\mathbf{x} - \mathbf{X}_{\ell})^{\top} \mathbf{H}^{-1} (\mathbf{x} - \mathbf{X}_{\ell}))}{\sum_{\ell=1}^n g((\mathbf{x} - \mathbf{X}_{\ell})^{\top} \mathbf{H}^{-1} (\mathbf{x} - \mathbf{X}_{\ell}))} - \mathbf{x}$. This $\boldsymbol{\beta}_{\mathbf{H}}$ is known as the mean shift, since it is the difference between the current iterate and a weighted mean of all data points. For our stopping rule, we iterate the recurrence in Equation (4) until either we reach a maximum number of iterations (400) or that the distance between subsequent iterations is less than 0.001 times the minimal marginal IQR (interquartile range) of the input data. This heuristic stopping rule gives sensible results in most cases.

The result is a sequence of points $\{\mathbf{X}_{i,0}, \mathbf{X}_{i,1}, \dots\}$ which traces out a path, along the steepest ascent of the density gradient, from the data point \mathbf{X}_i to the mode of the associated data-rich region. The data-rich regions are the ‘basins of attraction’ of the density gradient ascent. If the data points are associated with the same mode, then they are considered to be members of the same cluster. Thus the number of clusters is equal to the number of these basins of attraction. For more details on mean shift and other forms of density-based clustering, see Chacón and Duong (2018, Section 6.2). A clustering of geospatial data is also known as regionalisation (Duque et al., 2007).

The result of the mean shift clustering on the $n = 93$ *G. yorkrakinensis* locations into 6 clusters is displayed on the left panel in Figure 9. Observe that we do not need to specify the number of clusters in advance, and the clusters can be of any arbitrary shape. These represent two important advantages over k -means clustering, which requires an a priori number of clusters, and whose cluster shapes are restricted to be (intersections of) ellipses. Cluster #4 (cyan crosses) is the most northerly and most separate from the other clusters. Cluster #2 (brown triangles) forms the most southerly cluster and is also well-separated. Points on the right edge of cluster #1 (red circles) and those on the left edge of cluster #3 (green squares) are close to together, and k -means clustering tends to assign them to the same cluster, whereas the directionality of the mean shift assigns them to different clusters. The two smallest clusters #5 (blue boxed crosses) and #6 (magenta asterisks) comprise only two and one locations, so these may belong to the larger clusters #2 and #1 respectively. Since the mean shift relies on the density gradient ascent paths, we overlay the quiver plot of the density gradient on the convex hulls of the mean shift clusters on the right of Figure 9. We observe that the gradient ascent arrows within each cluster are oriented towards the mode.

The commands for mean shift clustering are `tidy_kms` and `st_kms`. The output is similar to that for a single density estimate, except that the data points are returned rather than the estimation grid points, and that `estimate` indicates the estimated cluster label rather than the density estimate value.

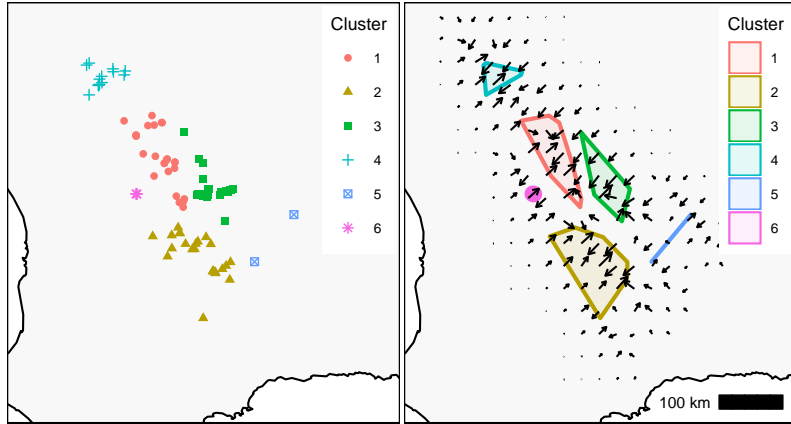


Figure 9: Mean shift clusters for *G. yorkrakinensis* ($n = 93$). (Left) Cluster members. (Right) Cluster convex hulls, superposed over the quiver plot of its density gradient estimate.

```
R> ## tidy mean shift clusters
R> t9 <- tidy_kms(yorkr_coord)
R> ggplot2::ggplot(t9, ggplot2::aes(x=lon, y=lat)) +
+   ggplot2::geom_point(ggplot2::aes(colour=estimate))
```

For geospatial data, the commands follow analogously.

```
R> ## geospatial mean shift clusters geom_sf plot
R> s9 <- st_kms(yorkr)
R> ggplot2::ggplot(s9) + ggplot2::geom_sf(ggplot2::aes(colour=estimate))
R> ## base R plot
R> plot(s9, pch=16)
```

Since the direction along which the data points are shifted is directly related to the density gradient, the default bandwidth for mean shift clustering in `tidy_kms` and `st_kms` is the plug-in bandwidth computed by `ks::Hpi(, deriv.order=1)`. For the *G. yorkrakinensis* data, this bandwidth matrix is $[4.39e8, -4.36e8; -4.36e8, 7.73e8]$. The bandwidth choice is made with the goal of optimal identification of the density gradient ascent paths. It is also supported by the results that the optimal bandwidth for estimating the mode of a density is closely related to the optimal bandwidth for density gradient estimation. In comparison, the optimal bandwidth matrix for the density estimate is $[8.84e8, -8.33e8; -8.33e8, 1.36e9]$. The difference reflects the added difficulty in the density gradient estimation problem.

5.2 Density ridge estimate

If a mode corresponds to the peak of single isolated mountain, then a ridge corresponds to the path that joins the multiple peaks in a mountain range. Ozertem and Erdogan (2011) proposes that the ridges of the density function serve as a generalisation of principal components. A density ridge, as its name suggests, forms a filament structure, in contrast to principal components which tend to form elliptical structures. Recall that the first principal component is determined by the eigenvector which corresponds to the largest eigenvalue of the variance matrix of the

data. On the other hand, a density ridge is based on the Hessian matrix of the density function f , which is comprised of the partial derivatives arranged in a 2×2 matrix

$$\mathbf{H}f = \begin{bmatrix} \partial^2 f / (\partial x_1^2) & \partial^2 f / (\partial x_1 \partial x_2) \\ \partial^2 f / (\partial x_1 \partial x_2) & \partial^2 f / (\partial x_2^2) \end{bmatrix}.$$

As all eigenvalues of the density Hessian matrix are negative near a ridge, we focus on the smallest eigenvalue.

Ozertem and Erdogmus (2011) adapt the mean shift recurrence to estimate the density ridge, by replacing the density gradient estimate $\mathbf{D}\hat{f}_{\mathbf{H}}$ by the projected density gradient estimate $\hat{p}_{\mathbf{H}}(\mathbf{x}) = \mathbf{u}_2(\mathbf{x})\mathbf{u}_2(\mathbf{x})^\top \mathbf{D}\hat{f}_{\mathbf{H}}(\mathbf{x})$ where $\mathbf{u}_2(\mathbf{x})$ is the eigenvector associated with the smallest eigenvalue of the density Hessian estimate $\mathbf{H}\hat{f}_{\mathbf{H}}(\mathbf{x})$. The mean shift recurrence for the projected gradient for a candidate point \mathbf{x}_i is

$$\mathbf{x}_{i,k+1} = \mathbf{x}_{i,k} + \mathbf{u}_2(\mathbf{x}_{i,k})\mathbf{u}_2(\mathbf{x}_{i,k})^\top \boldsymbol{\beta}_{\mathbf{H}}(\mathbf{x}_{i,k}) \quad (5)$$

where $\boldsymbol{\beta}_{\mathbf{H}}$ is the non-projected mean shift from Equation (4). The result is a sequence of points $\{\mathbf{x}_{i,0}, \mathbf{x}_{i,1}, \dots\}$ which traces out a path, along the steepest ascent of the projected density gradient, from the candidate point \mathbf{x}_i to an associated end point on the density ridge. We apply Equation (5) to a grid of m initial candidate points $\mathbf{x}_1, \dots, \mathbf{x}_m$ to obtain a density ridge estimate. The heuristic stopping rule is the same as for non-projected mean shift, i.e., we iterate until we reach either 400 iterations or the distance between subsequent iterations is less than 0.001 times the minimal marginal IQR of the input data. For more details on density ridge estimates, see Chacón and Duong (2018, Section 6.3).

The density ridge estimate for the *G. paradoxa* locations is displayed in Figure 10 as the purple lines. It can be interpreted as the sequence of peaks in the data density or as the filament equivalent of the first principal component of the data density. This ridge estimate is obtained from a 151×151 grid of initial 22801 candidate points. This density ridge reflects a considerable reduction in the complexity of the original *G. paradoxa* locations, since the Ramer-Douglas-Peucker simplification in `sf::st_simplify` (Ramer, 1972, Douglas and Peucker, 2011) is applied.

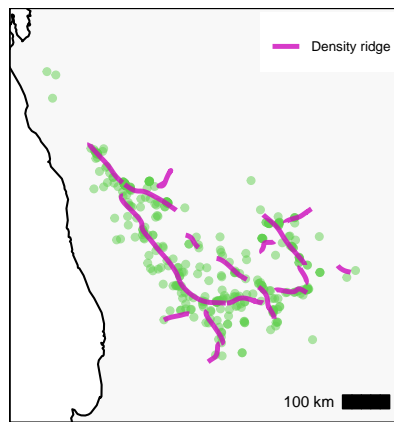


Figure 10: Density ridge estimates for *G. paradoxa* ($n = 358$), superposed on their locations.

The commands for the density ridge estimates are `tidy_kdr` and `st_kdr`. The output is similar to the output for a density estimate, except that the estimate grid points are replaced

by the points on the estimated density ridge, and the density estimate value is replaced by the density ridge indicator (`label`).

```
R> ## tidy density ridge estimate
R> t11 <- tidy_kdr(parad_coord)
R> ggplot2::ggplot(t11, ggplot2::aes(x=lon, y=lat)) +
+   ggplot2::geom_path(aes(colour=label, group=segment))

R> ## geospatial density ridge estimate geom_sf plot
R> s11 <- st_kdr(parad)
R> ggplot2::ggplot(s11) + ggplot2::geom_sf(aes(colour=label))
R> ## base R plot
R> plot(s11)
```

Since the direction along which the candidate points are shifted relies on the eigenvalue decomposition of the density Hessian estimate, the default bandwidth for a density ridge estimate in `tidy_kdr` and `st_kdr` is the plug-in bandwidth computed by `ks::Hpi(, deriv.order=2)`. For the *G. paradoxa* data, this bandwidth matrix is $[1.25\text{e}9, -6.90\text{e}8, -6.90\text{e}8, 8.16\text{e}8]$. For comparison, the optimal bandwidth matrix for the density estimate is $[1.03\text{e}9, -5.71\text{e}8, -5.71\text{e}8, 6.70\text{e}8]$. The difference reflects the added difficulty in the density Hessian estimation problem.

5.3 Significant density curvature regions

We return to kernel-based inference with feature significance. In this context, a ‘feature’ refers to an important characteristic of the density function f , such as a local mode (Godtliebsen et al., 2002). We focus on modal regions since these are data-rich regions, and which we characterise in terms of the local significance tests for the density curvature function $\mathbf{H}f$. At each candidate point \mathbf{x} , let the local null hypothesis be $H_0(\mathbf{x}) : \mathbf{H}f(\mathbf{x}) = 0$. The significant density curvature region is where the density curvature is significantly non-zero, and that the eigenvalues λ_1, λ_2 of $\mathbf{H}f$ are both negative:

$$\mathcal{M} = \{\mathbf{x} : \text{reject } H_0(\mathbf{x}), \lambda_1 f(\mathbf{x}), \lambda_2(\mathbf{x}) < 0\}.$$

A suitable local Wald test statistic for $H_0(\mathbf{x})$ is $W(\mathbf{x}) = \|\mathbf{S}(\mathbf{x})^{-1/2} \text{vech } \mathbf{H}\hat{f}_{\mathbf{H}}(\mathbf{x})\|^2$, where $\text{vech } \mathbf{H}\hat{f}_{\mathbf{H}} = [\partial^2 \hat{f}_{\mathbf{H}} / \partial x_1^2, \partial^2 \hat{f}_{\mathbf{H}} / (\partial x_1 \partial x_2), \partial^2 \hat{f}_{\mathbf{H}} / \partial x_2^2]$ are the unique elements of the estimate of the density Hessian matrix, and \mathbf{S} is the null variance of W . The formula for \mathbf{S} is given by Duong et al. (2008), and these authors also assert that the asymptotic null distribution of $W(\mathbf{x})$ is approximately chi-squared with 3 d.f. for all 2-dimensional candidate points \mathbf{x} .

Similar to the situation for the serially correlated hypothesis tests for the significant density difference regions in Section 3, we apply the Hochberg procedure to control for the overall level of significance. The estimate of the significant density curvature regions \mathcal{M} is

$$\hat{\mathcal{M}} = \{\mathbf{x} : \text{reject } H_0(\mathbf{x}), \hat{\lambda}_1 f(\mathbf{x}), \hat{\lambda}_2(\mathbf{x}) < 0\}$$

where $\hat{\lambda}_1, \hat{\lambda}_2$ are the eigenvalues of the estimate of density Hessian $\mathbf{H}\hat{f}_{\mathbf{H}}$ and are computed using the usual singular value decomposition.

In Figure 11, the significant density curvature regions for *G. paradoxa* are the orange regions. They are superposed on the density ridge estimate (purple curves). The significant density

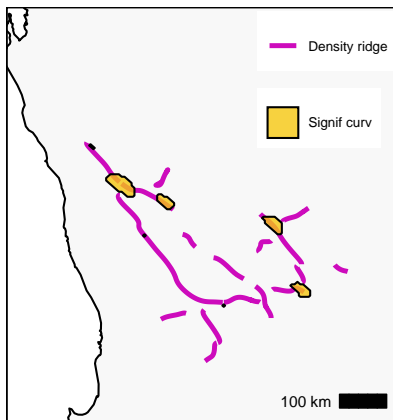


Figure 11: Significant density curvature regions for *G. paradoxa* ($n = 358$), superposed on their density ridge estimate.

curvature regions are 2-dimensional regions which tend to be concentrated at the most data-rich regions of the 1-dimensional filaments of the density ridge estimate.

The commands for the significant density curvature regions are `tidy_kfs` and `st_kfs`. The output is similar to the output for a density estimate, except that the density estimate value is replaced by the local Wald test statistic, and `label` is a significant density curvature indicator.

```
R> ## tidy significant modal regions
R> t12 <- tidy_kfs(parad_coord)
R> ggplot2::ggplot(t12, ggplot2::aes(x=lon, y=lat)) +
+   geom_contour_filled_ks(fill=7, colour=1)

R> ## geospatial significant modal regions geom_sf plot
R> s12 <- st_kfs(parad)
R> ggplot2::ggplot(s12) + ggplot2::geom_sf(fill=7)
R> ## base R plot
R> plot(s12, col=7)
```

Since the local Wald test statistics depend on the density Hessian estimate, the default bandwidth for a density ridge estimate in `tidy_kfs` and `st_kfs` is the plug-in computed by `ks::Hpi(, deriv.order=2)`. For the *G. paradoxa* data, this bandwidth matrix is $[1.25\text{e}9, -6.90\text{e}8, -6.90\text{e}8, 8.16\text{e}8]$.

6 Export to external GIS software

The ability to export the geospatial kernel estimates in standard geospatial data formats via the `sf::write_sf` function extends the functionality of the `eks` package in true GIS software. For example, the commands to export the *G. yorkrakinensis* locations `yorkr`, the polygons of the quartile probability contour regions of the density estimate `s1`, and the `grid` field of the rectangular polygons for the estimation grid of `s1` to the geopackage format are:

```
R> ## export to external geospatial format
R> sf::write_sf(yorkr, dsn="grevillea.gpkg", layer="yorkrakinensis")
```

```
R> sf::write_sf(st_get_contour(s1), dsn="grevillea.gpkg",
+   layer="yorkrakinensis_cont")
R> sf::write_sf(s1$grid, dsn="grevillea.gpkg", layer="yorkrakinensis_grid")
```

The `grevillea.gpkg` geopackage consists of three layers: `yorkrakinensis` for the point geometries of the *G. yorkrakinensis* locations, `yorkrakinensis_cont` for the multi-polygons of the quartile contour regions of the density estimate, and `yorkrakinensis_grid` for the rectangular polygons of the estimation grid.

Recall that quiver plots can be difficult to produce with geospatial data in `ggplot2` graphics, since the arrows require trial and error to display suitably with `ggplot2::geom_segment`. In contrast, quiver plots are straightforward in a GIS software, e.g. QGIS (QGIS.org, 2021), where rescaleable arrows are a native feature. We can export the `sf` field of the output from `st_kdde(, deriv_order=1)` using

```
R> sf::write_sf(s1$sf, dsn="grevillea.gpkg", layer="yorkrakinensis_quiver")
```

This `grevillea.gpkg` geopackage can be subsequently employed in QGIS, which is an industry standard software for GIS practitioners since it offers features that are not available in R. For example, it has an interactive point-and-click interface, and it incorporates fast rendering of the OpenStreetMap base maps. A screenshot from a QGIS analysis for a quiver plot overlaid on a density estimate is given in the left panel of Figure 12, with a similar symbology to those in Figure 8, i.e., the quartile probability contours of the density estimate are in a heat colour scale, and the arrows of the quiver plot of the density gradient estimate are in black.

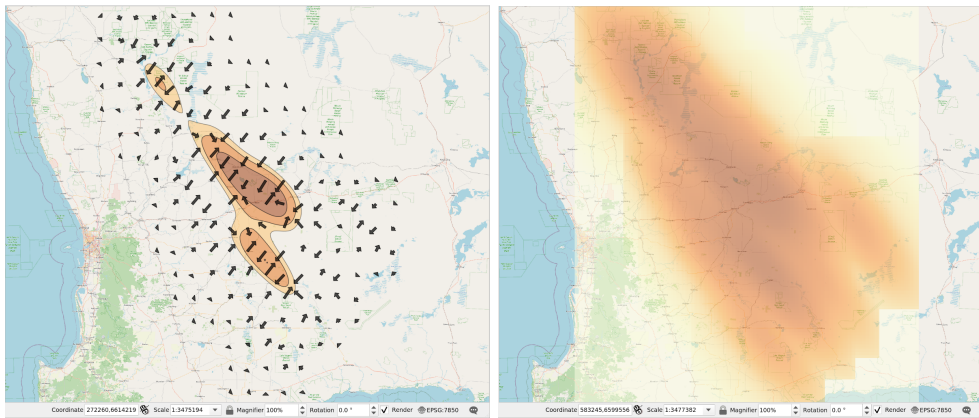


Figure 12: Screenshots of QGIS analysis for *G. yorkrakinensis* ($n = 93$). (Left) Probability contour plot of density estimate and quiver plot of density gradient estimate. (Right) Raster of density estimate.

In addition, QGIS efficiently handles raster geospatial data: rasters are the geospatial equivalent of image data. Whilst the `grid` field of a kernel estimate consists of the rectangular polygons for each pixel of the estimation grid, it is converted to a raster via the `stars` package. The converted raster is displayed on the right of Figure 12.

```
R> stars::write_stars(stars::st_rasterize(s1$grid),
+   dsn="yorkrakinensis_raster.tif")
```

7 Other data analysis settings

There are numerous variations on the standard density estimate provided by `tidy_kde` for tidy data. For bounded data, there is a boundary density estimate (`tidy_kde_boundary`) and a truncated density estimate (`tidy_kde_truncate`). To allow for the kernel function and/or the bandwidth matrix to vary, there are the sample point density estimate (`tidy_kde_sp`) and balloon density estimate (`tidy_kde_balloon`). For data observed with errors, there is the deconvolved density estimate (`tidy_kdcde`). There are also distribution-based estimates, with a cumulative distribution estimate (`tidy_kcde`), a copula estimate (`tidy_kcopula`), and a ROC (receiver operating characteristic) curve (`tidy_kroc`). These are all also implemented for geospatial data as `st_k*`. All of these utilise the appropriate default bandwidth selector from the `ks` package. For brevity, we do not illustrate them here: their usage is demonstrated in their help pages contained in the `eks` package.

Tidy kernel smoothers also are applicable to tidy univariate data. A density estimate of the longitude coordinates of *G. yorkrakinensis* is shown in Figure 13, with the rug plot on the horizontal axis.

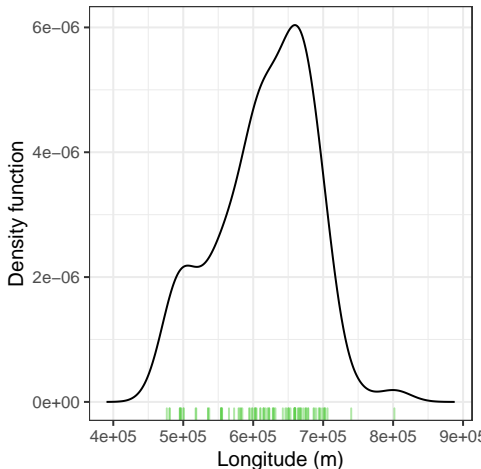


Figure 13: Density estimate of the *G. yorkrakinensis* ($n = 93$) longitude coordinates, with their rug plot.

The same command `tidy_kde` can be employed for 1-dimensional data input to compute the density estimate. The `ggplot2::ggplot` method for `tidy_ks` objects adds the default aesthetic mapping `ggplot2::aes(y=estimate, weight=ks)`, as well as a default vertical axis label, in this case "Density function". The appropriate layer function to display the 1-dimensional density estimate is `ggplot2::geom_line`. A rug plot is added using the layer function `geom_rug_ks`.

```
R> ## tidy 1D density estimate
R> t13 <- tidy_kde(dplyr::select(yorkr_coord, lon))
R> ggplot2::ggplot(t13, ggplot2::aes(x=lon)) +
+   ggplot2::geom_line(colour=1) + geom_rug_ks(colour=3)
```

The default bandwidth computed by `ks::hpi` is 2.32e4, which is the standard deviation of the univariate kernel function. In contrast, the bivariate bandwidth [8.84e8, -8.33e8; -8.33e8,

1.36e9] computed by `ks::Hpi` is the variance matrix of the bivariate kernel function. All univariate bandwidths are named in the same way as the bivariate bandwidths, except that the capital `H` is replaced by a lower case `h`, e.g., `ks::hns` for the normal scale, `ks::hucv` for the unbiased cross validation and `ks::hscv` for the smoothed cross validation bandwidths.

8 Conclusion

We have introduced a new R package `eks` which serves as a bridge from the comprehensive suite of kernel smoothers in the `ks` package to the tidyverse and geospatial analysis. A wide range of kernel smoothing methods are now available, which (i) improve on the existing kernel density estimates, and (ii) improve the accessibility to more complex kernel-based data analyses, such as density-based classification (supervised learning), mean shift clustering (unsupervised learning), significant density difference testing, density derivative estimation, density ridge estimation and significant modal region testing. The `eks` package provides practitioners with additional tools to create compelling statistical visualisations from kernel smoothers, whether they are using tidy or geospatial data, or whether they are using base R or tidyverse graphics.

References

Baddeley, A. and Turner, R. (2005). spatstat: An R package for analyzing spatial point patterns. *Journal of Statistical Software*, 12(6):1–42.

Baillo, A. and Chacón, J. E. (2021). Chapter 1 - statistical outline of animal home ranges: An application of set estimation. In Srinivasa Rao, A. S. and Rao, C., editors, *Data Science: Theory and Applications*, volume 44 of *Handbook of Statistics*, pages 3–37. Elsevier.

Beck, G., Duong, T., Azzag, H., and Lebbah, M. (2016). Distributed mean shift clustering with approximate nearest neighbours. In *Proceedings of the 2016 International Conference on Neural Networks (IJCNN)*, pages 3110–3115.

Béranger, B., Duong, T., Perkins-Kirkpatrick, S. E., and Sisson, S. A. (2019). Tail density estimation for exploratory data analysis using kernel methods. *Journal of Nonparametric Statistics*, 31:144–174.

Bowman, A. W. and Foster, P. (1993). Density based exploration of bivariate data. *Statistics and Computing*, 3:171–177.

Chacón, J. E. and Duong, T. (2010). Multivariate plug-in bandwidth selection with unconstrained bandwidth matrices. *Test*, 19:375–398.

Chacón, J. E. and Duong, T. (2018). *Multivariate Kernel Smoothing and Its Applications*. Chapman and Hall/CRC, Boca Raton.

Chacón, J. E., Duong, T., and Wand, M. P. (2011). Asymptotics for general multivariate kernel density derivative estimators. *Statistica Sinica*, 21:807–840.

Douglas, D. H. and Peucker, T. K. (2011). Algorithms for the reduction of the number of points required to represent a digitized line or its caricature. In Dodge, M., editor, *Classics in Cartography*, pages 15–28. John Wiley & Sons.

Duong, T. (2007). *ks*: Kernel density estimation and kernel discriminant analysis for multivariate data in R. *Journal of Statistical Software*, 21(7):1–16.

Duong, T. (2013). Local significant differences from nonparametric two-sample tests. *Journal of Nonparametric Statistics*, 25:635–645.

Duong, T. (2022). *eks: Tidy and Geospatial Kernel Smoothing*. R package version 1.0.2.

Duong, T., Cowling, A., Koch, I., and Wand, M. P. (2008). Feature significance for multivariate kernel density estimation. *Computational Statistics and Data Analysis*, 52:4225–4242.

Duong, T. and Hazelton, M. L. (2003). Plug-in bandwidth matrices for bivariate kernel density estimation. *Journal of Nonparametric Statistics*, 15:17–30.

Duque, J. C., Ramos, R., and Suriñach, J. (2007). Supervised regionalization methods: A survey. *International Regional Science Review*, 30:195–220.

Evans, J. S. and Murphy, M. A. (2022). *spatialEco*. R package version 2.0-0.

Fukunaga, K. and Hostetler, L. (1975). The estimation of the gradient of a density function, with applications in pattern recognition. *IEEE Transactions on Information Theory*, 21:32–40.

Godtliebsen, F., Marron, J. S., and Chaudhuri, P. (2002). Significance in scale space for bivariate density estimation. *Journal of Computational and Graphical Statistics*, 11:1–21.

Hochberg, Y. (1988). A sharper Bonferroni procedure for multiple tests of significance. *Biometrika*, 75:800–802.

Hyndman, R. J. (1996). Computing and graphing highest density regions. *American Statistician*, 50:120–126.

Kalair, K. and Connaughton, C. (2021). Anomaly detection and classification in traffic flow data from fluctuations in the flow–density relationship. *Transportation Research Part C: Emerging Technologies*, 127:103178.

Myers, N., Mittermeier, R. A., Mittermeier, C. G., Da Fonseca, G. A. B., and Kent, J. (2000). Biodiversity hotspots for conservation priorities. *Nature*, 403:853–858.

OGC (2021). Simple feature access. Open Geospatial Consortium. <https://www.ogc.org/standards/sfa>.

O'Hara-Wild, M. (2019). *ggquiver: Quiver Plots for 'ggplot2'*. R package version 0.2.0.

Ozertem, U. and Erdoganmus, D. (2011). Locally defined principal cruves and surfaces. *Journal of Machine Learning Research*, 12:1249–1286.

Pebesma, E. (2018). Simple features for R: Standardized support for spatial vector data. *The R Journal*, 10:439–446.

QGIS.org (2021). *QGIS Geographic Information System*. QGIS Association.

Ramer, U. (1972). An iterative procedure for the polygonal approximation of plane curves. *Computer Graphics and Image Processing*, 1:244–256.

Rudis, B., Bolker, B., and Schulz, J. (2017). *ggalt: Extra Coordinate Systems, 'Geoms', Statistical Transformations, Scales and Fonts for 'ggplot2'*. R package version 0.4.0.

Schauer, K., Duong, T., Bleakley, K., Bardin, S., Bornens, M., and Goud, B. (2010). Probabilis-

tic density maps to study global endomembrane organization. *Nature Methods*, 7:560–568.

Wickham, H. (2014). Tidy data. *Journal of Statistical Software*, 59(10):1–23.

Wickham, H. (2016). *ggplot2: Elegant Graphics for Data Analysis*. Springer-Verlag, New York.